Robust Energy Management Optimization for PHEB Considering Driving Uncertainties by Using Sequential Taguchi Method

Xiaodong Sun, *Senior Member, IEEE,* Zongzhe Chen, Mingzhang Pan, Yingfeng Cai, *Senior Member, IEEE,* Zhijia Jin, Gang Lei, *Senior Member, IEEE,* and Xiang Tian

***Abstract*—In this paper, a robust optimization design method is presented to improve the energy management effect of plug-in hybrid electric buses (PHEB). Various uncertain factors are taken into account, including passenger load, resistance, and efficiency. First, the deterministic design of the energy management strategy is conducted under a city bus route, which is divided into 20 segments according to bus stations. The segmented equivalent consumption minimization strategy (ECMS) is established wherein the equivalent factors undergo optimization by the dynamic programming (DP) algorithm. Then, the sequential Taguchi method is utilized to optimize the equivalent factors based on deterministic results. Uncertain factors are designated as noise factors, while equivalent factors serve as control factors. The total fuel consumption is chosen as the optimization objective, with consideration given to the final state of charge (SOC) limit. The simulation results demonstrate that the energy management system obtained by robust optimization achieves a 1.9% reduction in fuel consumption expectation compared to the deterministic optimization. The result proves the validity of the proposed robust optimization method.**

***Index Terms*—Plug-in hybrid electric bus, Energy management, Taguchi robust design, Equivalent consumption minimization strategy**

I. INTRODUCTION

Nowadays, pressure from both energy crises and environmental pollution promotes the development of plug-in hybrid electric vehicles (PHEV). Compared to conventional vehicles, an additional power source increases the freedom of power distribution which allows the engine to operate in a high-efficiency range [1]. Regenerative braking further improves fuel economy as well [2]. The ability to charge from the grid enables PHEV to work for long distances only using electricity. In public transport areas, the plug-in hybrid electric bus (PHEB) has been adopted in many cities [3, 4].

Manuscript received 29 Jun. 2024; revised 27 Sep. 2024; accepted 5 Oct. 2024. This work was supported by the National Natural Science Foundation of China under Project 52225212. (*Corresponding author: Mingzhang Pan*)

X. Sun, Z. Chen, Y. Cai, Z. Jin, and X. Tian are with the Automotive Engineering Research Institute, Jiangsu University, Zhenjiang 212013, China (email: xdsun@ujs.edu.cn, 2212204054@stmail.ujs.edu.cn, yfcai@ujs.edu.cn, 2111904009@stmail.ujs.edu.cn, and 1000004966@ujs.edu.cn).

M. Pan is with the College of Mechanical Engineering, Guangxi University, Nanning 530004, China (email: pmz@gxu.edu.cn).

G. Lei is with the School of Electrical and Data Engineering, University of Technology Sydney, NSW2007, Australia (e-mail: Gang.Lei@uts.edu.au).

The energy management strategy directly determines the fuel efficiency and emission performance of PHEBs. The current energy management strategies can be broadly classified into four categories, namely rule-based energy management strategy [5, 6], global optimization energy management strategy [7, 8], instantaneous optimization energy management strategy [9, 10], and learning-based energy management strategy [11]. Each approach exhibits distinctive characteristics. The global optimization method can achieve theoretically optimal energy management performance when the entire driving cycle is known beforehand. Subject to substantial computational demands, the global optimization method is utilized to assess the control effectiveness of other strategies [12], provide offline optimization results as the basis for online control [13], and solve the optimal control law under short-range vehicle speed prediction [14]. From the standpoint of real-time control, rule-based energy management strategies are widely adopted in the industry owing to elevated reliability and low computing cost [15]. However, optimal control remains a formidable challenge for the rule-based method [16]. Learning-based methods can obtain the near-optimal solution [17]. However, the relatively large computing load and parameter scale restrict the practical application. In response to both real-time and optimal control requirements, the instantaneous optimization method emerges as a viable alternative. By minimizing the transient cost function at each moment, a discernible control effect approximating global optimization is realized [18]. Representative strategies include the equivalent consumption minimization strategy (ECMS) and Pontryagin's minimum principle (PMP) [19-21]. Considering the segment characteristic of the PHEB driving cycle, segmented ECMS assigns different control parameters to each road segment for better fuel economy. In [22], the offline optimization of control parameters for segments is conducted with different initial state of charge (SOC). The results are converted to a look-up table for real-time adjustments. Model prediction control is applied to make adaptive changes in ECMS based on road segments [23].

In deterministic optimization design, all operating parameters are fixed at their nominal values without any variation. The energy management strategy optimized under this approach can achieve theoretically optimal given the known driving cycle. However, uncertain factors such as passenger load exhibit continuous variability, leading to a changing and unpredictable demand for power. Consequently, the control effect of energy management experiences degradation. Given the potential for considerable variations in the gross mass of PHEB due to large passenger capacity, numerous robust design methods have been proposed [24-29].

Robust design aims to find an optimal solution that is insensitive to noise. The Taguchi robust design and design for six sigma (DFSS) are representative methods. The Taguchi robust design is widely used in manufacturing, engineering, product design, and other technological process [30-32]. In [24], the Taguchi method is utilized to design a robust co-state sequence of PMP, considering uncertain driving cycles and vehicle mass. In [25], the parameters of the proportion-integration (PI) controller are designed through the Taguchi method. DFSS is generally used to develop products to meet needs with very low defect levels [26]. As reported in [27], a robust co-state for pattern recognition-based energy management is found offline through DFSS.

The above optimization methods address the impact of uncertain factors, encompassing passenger load and driving cycle. Notably, additional parameters also exhibit uncertainty during actual driving. Regarding power demand, both rolling resistance and air drag coefficient fluctuate within a narrow range. During operation, the efficiency of the machine and engine may differ from the nominal value [33, 34]. In the context of long-term operation, variations in uncertainties can lead to changes in energy management performance. The accumulation of different uncertainties will make the control effect further deviate from the expectation.

This paper aims to enhance the fuel economy of PHEB during long-term operation by robust energy management optimization. For real-time implementation on a city bus route, the segmented ECMS is selected. Additionally, the sequential Taguchi robust method is employed to identify robust equivalent factors. The primary innovations of this study include two aspects:

1) Sequential Taguchi robust optimization is conducted based on deterministic optimization. The optimized energy management strategy can achieve lower fuel consumption when facing driving uncertainties.

2) Various uncertainties during actual driving, including air drag resistance, rolling resistance, passenger load, and efficiency attenuation of power source are comprehensively considered. During long-term operation, the segmented ECMS after robust optimization demonstrates superior practical performance.

This paper is organized as follows. In Section II, the PHEB model is established. Section III presents the formulation of segmented ECMS, deterministic optimization, and robust optimization utilizing the sequential Taguchi method. The simulation and test are conducted, and the results are analyzed in Section IV. Conclusions are drawn in Section V.

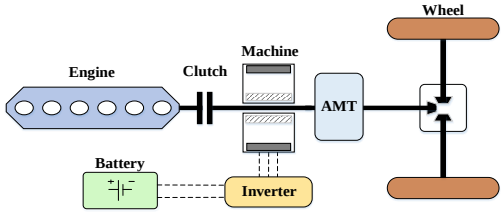

Fig. 1. Structure of the PHEB.

II. PHEB MODEL

The PHEB in this study adopts a coaxial configuration, where torque from both the engine and machine is transmitted to the same shaft, so the total power belongs to mechanical power. The structure of PHEB in this paper is shown in Fig. 1.

A. *Vehicle Dynamic Model*

Considering that the primary purpose of energy management strategy is to minimize fuel consumption while satisfying power requirements, the longitudinal dynamics can be used as the theoretical basis for modeling. The driving torque acting on the wheels T_w, which originates from the coupling torque can be formulated as

$$T_w = (T_e + T_m) i_{AMT} i_f \eta_t \tag{1}$$

where T_e and T_m are the engine torque and machine torque. i_{AMT} and i_f are the ratio of AMT and final drive respectively. η_t is the transmission efficiency. Meanwhile, resistant torque T_f can be written as

$$T_f = (MgC_r \cos\theta + \frac{1}{2}\rho_a A C_d v^2 + Mg\sin\theta + \delta M \frac{dv}{dt}) \cdot r + T_b \tag{2}$$

where M is the total mass including curb mass and passenger load. g is the local gravity acceleration. C_r and C_d are the rolling resistance coefficient and air drag coefficient. θ, ρ_a, A, v, and δ represent the road angle, air density, bus frontal areas, speed, and rotational mass conversion factor. r is the radius of the wheels. T_b represents mechanical braking torque. For longitudinal dynamic balance, T_w should be equal to T_f. The main parameters of the PHEB are given in Table I.

TABLE I
PARAMETER OF THE PHEB

Component	Parameter	Value
Vehicle	Rolling resistance coefficient	0.016
	Air drag coefficient	0.6
	Front area	6.05
	Curb mass	13000kg
	Gross mass	16500kg
	Wheel radius	0.512m
Engine	Type	6.5L, diesel engine
	Maximum torque	1150Nm
	Maximum power	250kW
Machine	Type	PMSM
	Maximum torque	870Nm
Battery	Voltage	390V
	Capability	26.6kWh
AMT	Gear ratios	6.71/3.77/2.26/1.44/1/0.77
Final drive	Transmission ratio	5.571

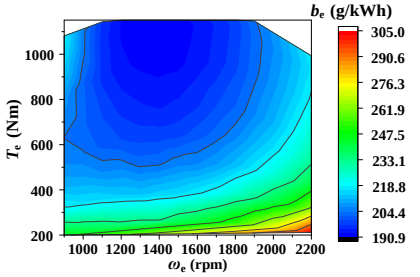

Fig. 2. Fuel consumption map of diesel engine.

B. Engine Model

The energy management strategy prioritizes fuel consumption over the specific combustion conditions or the internal operating state of the engine components. Therefore, a simplified quasi-static engine model is necessary. The instantaneous fuel consumption $\dot{m}_f$ can be calculated through

$$\dot{m}_f = \frac{T_e \omega_e}{9550} \cdot \frac{b_e}{3600} \tag{3}$$

where ω_e and b_e represent the rotational speed of the engine and the fuel consumption rate. Once ω_e and T_e are known, b_e can be obtained through looking up the fuel consumption contour map shown in Fig. 2.

C. Electric Machine Model

PHEB is equipped with one permanent magnet synchronous machine (PMSM) which has two working modes. During the braking process, the electric machine can regenerate electricity by operating as a generator. When the PHEB requires driving force, torque from the electric machine in motor mode helps adjust the engine operating points.

Corresponding to different working modes, the machine power can be formulated as

$$P_m = \begin{cases} \dfrac{T_m \omega_m}{\eta_m} & T_m > 0 \\ T_m \omega_m \eta_m & T_m < 0 \end{cases} \tag{4}$$

where P_m, ω_m, and η_m represent the machine power, the rotational speed of the machine, and the efficiency of the machine. Negative torque indicates that the electric machine is charging the battery. Similar to the fuel consumption rate, η_m can be deterministic by a look-up table quickly according to T_m and ω_m. The electric machine efficiency map used in this paper is shown in Fig. 3.

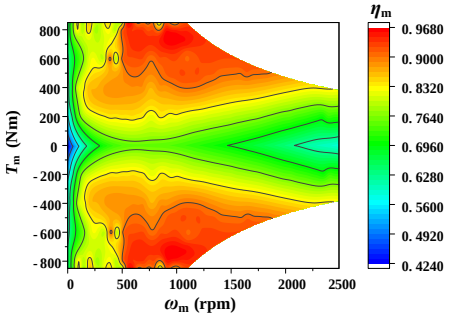

Fig. 3. Electric machine efficiency map.

D. Battery Model

In this paper, a simplified equivalent internal resistance battery model is selected to simulate the complex dynamic characteristics, as shown in Fig. 4. The effects of battery aging and temperature change are ignored as well.

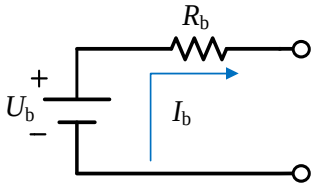

Fig. 4. The simplified schematic of the battery.

Battery current and SOC can be calculated by

$$I_b = \frac{U_b - \sqrt{U_b^2 - 4R_b P_b}}{2R_b} \tag{5}$$

$$soc = \frac{Q_b - \int_0^T I_b dT}{Q_b} \tag{6}$$

where I_b and soc are battery current and SOC. P_b, U_b, R_b, and Q_b represent the battery power, open circuit voltage, internal resistance, and nominal battery capacity, respectively. As SOC decreases, both R_b and U_b change accordingly. The characteristics of the battery are shown in Fig. 5.

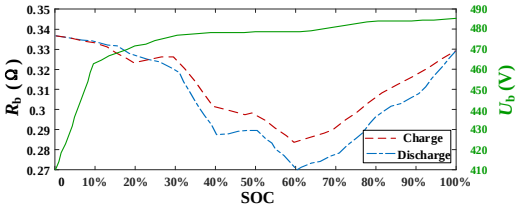

Fig. 5. The schematic diagram of battery characteristics.

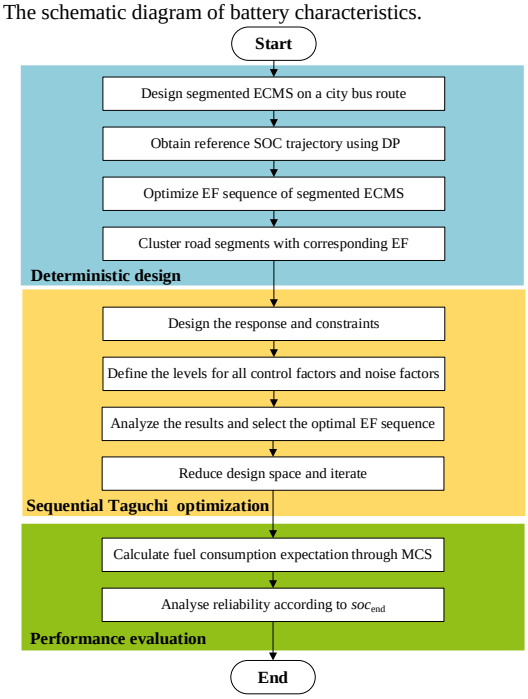

Fig. 6. Produce of robust energy management optimization.

III. Robust Energy Management Optimization

The proposed robust energy management strategy can be divided into three steps: (i) Deterministic energy management strategy design, (ii) sequential Taguchi robust optimization, and (iii) Performance evaluation, as shown in Fig. 6. Segmented ECMS is selected as the foundational energy management strategy. It should be noted that the equivalent factors (EF) vary between bus stations for better control.

A. Deterministic design of segmented ECMS

The principle of ECMS is to allocate a portion of energy consumption to electricity at each moment, equating the consumed electricity to a corresponding amount of fuel. The instantaneous equivalent fuel consumption can be calculated through

$$\dot{m}_{f,eqv}(t) = \dot{m}_f(t) + \dot{m}_{ress}(t) \tag{7}$$

$$\dot{m}_{\text{ress}}(t)=\frac{s(t)}{Q_{\text{lhv}}}P_{\text{b}}(t) \tag{8}$$

where Q_{lhv}, $\dot{m}_{\text{f,eqv}}(t)$ and $\dot{m}_{\text{ress}}(t)$ represent the fuel low calorific, the instantaneous equivalent fuel consumption, and the electricity equivalent fuel consumption. $s(t)$ represents EF which functions to allocate a specific cost to the utilization of electricity, thereby directly influencing the control effect of ECMS.

This paper focuses on a PHEB operating on a city bus route. The route has a total length of 11.6 km and 21 bus stations, as shown in Fig. 7.

Fig. 7. A city bus route for PHEB.

In previous work, historical driving information on this route was collected. After cluster analysis of original data, one representative driving cycle is built for ECMS design, including reference passenger numbers between bus stations, as shown in Fig. 8. Due to the varying number of passengers on each trip and the differing speed characteristics across regions, the entire driving cycle is divided into 20 segments with bus stations serving as nodes. Accordingly, each segment is assigned a specific EF, which is the key to segmented ECMS. In real-time driving, the energy management system of PHEB adjusts the EF dynamically based on the current bus station.

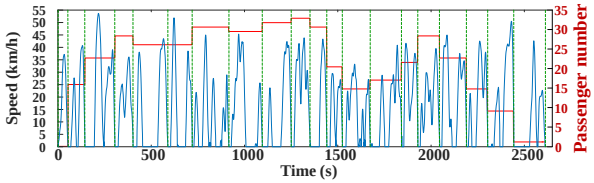

Fig. 8. The constructed driving cycle of a city bus route.

The SOC trajectory obtained from dynamic programming (DP) serves as a reference for deterministic optimization. The objective is to minimize deviations between the reference SOC trajectory and the SOC trajectory generated by ECMS. Table II lists the deterministic optimization result.

In the sequential Taguchi robust optimization, employing 20 EFs as optimization variables will result in a substantial number of tests and a large orthogonal table. Therefore, segments of the constructed driving cycle are clustered to reduce the complexity and difficulty of robust optimization. The K-means method is utilized, and the characteristic parameters selected include mean speed, mean running speed and speed standard deviation.

TABLE II
DETERMINISTIC OPTIMIZATION RESULTS

No	EF	No	EF	No	EF	No	EF
1	2.73	6	2.99	11	3.17	16	3.90
2	2.11	7	3.03	12	2.94	17	3.80
3	3.79	8	3.89	13	1.82	18	3.13
4	2.86	9	3.83	14	2.86	19	3.58
5	3.79	10	3.67	15	3.94	20	2.68

The 20 segments are clustered into four types. Additionally, EFs within each of the four types are close in value, which indicates the validity of clustering. Based on the deterministic optimization result, the mean EF of each segment type can be calculated, and this mean value is then assigned to all segments within the particular type. Consequently, four EFs corresponding to segment types are derived, namely S_1, S_2, S_3, and S_4. The deterministic optimization results after clustering are listed in Table III, and Fig. 9 illustrates the deterministic EF sequences.

TABLE III
DETERMINISTIC SOLUTION AFTER CLUSTERING

Segment type	1	2	3	4
EF	S_1	S_2	S_3	S_4
Value	3.05	3.80	2.78	1.97

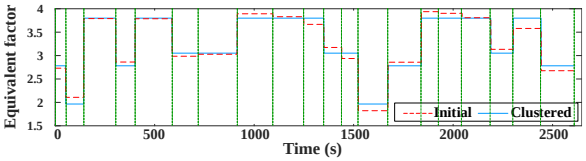

Fig. 9. Deterministic EF sequences.

B. *Uncertainties during driving*

During actual driving, the parameters of PHEB may fluctuate around their corresponding nominal values. Uncertainties from many aspects are taken into account in the process of robust optimization.

1) Passenger load

While PHEB operates on a city bus route, the number of passengers will inevitably fluctuate, thereby influencing the actual performance of the energy management system. Therefore, passenger load is selected as an uncertain factor, denoted by M_{p}.

The distribution of passenger flow is a specialized issue characterized by uneven distribution in time and space. The specific distribution and temporal changes in passenger flow are not the primary focus of this paper. For simplicity, it is assumed that the number of passengers between stations conforms to a normal distribution. The mean passenger number of each road segment is shown in Fig. 8. Additionally, the average passenger weight is 70kg.

2) Rolling resistance

The PHEB must overcome rolling resistance while traversing the relatively flat urban road surface. When estimating the required power for a PHEB, the rolling resistance coefficient C_{r} is typically considered at its nominal value. However, C_{r} is influenced by road surface type, driving speed, tire pressure, etc., which vary with time and segments during the actual driving process, leading to uncertainty of rolling resistance.

3) Air drag resistance

In deterministic design, PHEB is usually considered as operating under windless conditions where the air drag coefficient C_{d} remains constant. Although C_{d} is mainly deterministic by the body configuration, uncertainties such as the distance from the ground, pitch angle, and lateral wind matter as well. Besides, C_{d} remains constant only at higher vehicle speeds, elevated dynamic pressures, and when the corresponding gas viscosity is relatively low. Therefore, the air drag resistance coefficient is selected as one uncertain factor.

4) Attenuation of machine and engine efficiency

The power source of a PHEB comprises an engine and a machine, the efficiency of which is determined by the current speed and the torque. However, factors like abrasion, components aging, and changing operating conditions can cause the attenuation of efficiency. Consequently, the actual efficiency of the power source may be lower than the expected value, directly affecting energy management decisions. Over time, the error continues to accumulate. Hence attenuation of motor and engine efficiency are selected as uncertain factors, denoted by attenuation coefficients σ_m and σ_e.

All uncertain factors considered in this paper are listed in Table IV. Given the relatively stable nature of urban driving conditions, uncertainties are presumed to follow normal distributions with small standard deviations. During each actual driving cycle, the uncertainties fluctuate randomly.

TABLE IV
NOMINAL VALUE AND STANDARD DEVIATIONS OF UNCERTAINTIES

Parameter	Nominal values	Standard deviations
C_r	0.016	0.001
C_d	0.6	0.02
σ_m	0.97	0.0045
σ_e	0.97	0.0045
M_p	2/16/22/27/25/25/29/28/30/31 /29/20/15/17/21/27/22/15/10/3	2/9/10/12/13/10/9/6/7/6 /9/8/10/7/8/9/10/7/8/2

C. Sequential Taguchi robust optimization

By utilizing the orthogonal array matrix and statistical analysis, the Taguchi method empowers engineers to efficiently identify the most influential factors, optimize design parameters, and enhance the overall quality. A sequential Taguchi method, combining the strengths of the Taguchi method and the sequential optimization strategy, is applied to systematically search for a robust solution. The robust optimization method in this paper can be divided into seven 7 steps:

Step 1: Determine the response and constraints of the sequential Taguchi method.

The optimization model is defined as

$$\begin{aligned} \min: \quad & f(x_s) = \omega_1 m_f + \omega_2 \left| soc_{end} - 30\% \right| \\ \text{s.t.} \quad & g_{c1}(x_s) = 30\% \le soc_{end} \le 35\% \\ & g_{c2}(x_s) = T_m \in [T_{m\min}, T_{m\max}] \\ & g_{c3}(x_s) = T_e \in [T_{e\min}, T_{e\max}] \\ & g_{c4}(x_s) = \omega_m \in [\omega_{m\min}, \omega_{m\max}] \\ & g_{c5}(x_s) = \omega_e \in [\omega_{e\min}, \omega_{e\max}] \end{aligned} \tag{9}$$

where x_s, f, m_f, and g_c are the control factor, response, total fuel consumption, and constraint, respectively. soc_{end} represents the final SOC. ω_1, ω_2 are the weight factors. The total fuel consumption of PHEB after 5 successive trips on the city bus route is selected as the response, with punishment that final SOC deviates from the lower limit of 30%. Additionally, 35% is set as the upper limit of SOC to avoid insufficient battery usage. To prevent over-discharge, an additional charge-sustaining (CS) mode is designed.

Step 2: Select control and noise factors.

Four EFs corresponding to segment types are chosen as control factors. To account for the influence of uncertainty on the PHEB energy management strategy, noise factors consist of uncertain factors shown in Table IV.

Step 3: Define the levels for control factors and noise factors.

Both the control factor and the noise factor are designed at 3 levels. For each control factor, level 2 represents the initial value, which is the result of deterministic optimization listed in Table III. The step size is set as 0.4 in the first iteration, determining level 1 and level 3. As for the noise factors, nominal values μ in Table IV correspond to level 2. Analogously level 1 and level 3 correspond to μ+1.5σ and μ-1.5σ where σ represents the standard deviation.

Step 4 Design of the inner-outer table and implement the simulation.

The $L_9(3^4)$ inner orthogonal array is generated by control factors. Each row represents a unique combination of control factor levels. Similarly, the $L_{16}(3^5)$ outer orthogonal array has 16 rows representing different noise conditions. During one iteration, 144 (9×16) simulations of combinations will be executed.

Step 5 Compute the S/N ratio and select the best level of each EF.

According to the data obtained from the simulation, the signal/noise (S/N) ratio can be utilized as an evaluation index to find the optimal combination of EFs. Two main steps should be accomplished to calculate the S/N ratios of each level. Lower fuel consumption signifies a better energy management effect. Hence, the smaller-the-better criterion is applied, where a higher S/N ratio signifies less fuel consumption and better robustness. First, the S/N ratio for each row of the inner orthogonal array is calculated by

$$SN(i) = -10 \times \lg[\sum_{j=1}^{16} f^2(i,j)] \tag{10}$$

where i (1,2…9) and j (1,2…16) are the row numbers of the inner and outer table respectively. $f(i,j)$ denotes the response of the corresponding simulation results.

Then, the average S/N ratio for all levels of EFs is calculated based on SN(i). The S/N ratio of a level is determined by simulation with EF set at this level. For example, the S/N ratio for level 1 of S_2 is the average of SN(1), SN(4), and SN(7).

The level revealing the highest S/N ratio of each control factor is selected as the outcome. As illustrated in Fig. 10, levels 3, 2, 1, and 2 are selected for S_1, S_2, S_3, and S_4 in iteration 1. Table V lists the corresponding selection results in bold.

Step 6 Calculate the value of the optimization function of the selected EF combination.

The sequential Taguchi method involves multiple iterations of a single Taguchi design. The introduction of the iteration mechanism ensures the convergence of the optimization process and guarantees that the final EF sequence cannot be further optimized. Fig. 11 illustrates the flowchart, where steps 3 to 5 are considered as one iteration process. The optimization function for the selected EF combination in each iteration can measure the robust optimization effect, which is defined as

$$F = \frac{1}{16} \times \sum_{j=1}^{16} f(j) \tag{11}$$

where F denotes the value of the optimization function. $f(j)$ refers to the response of selected EFs with noise factors in the outer table, row j.

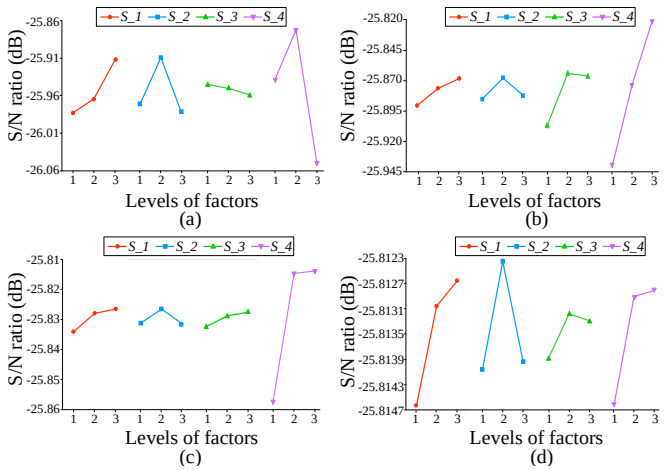

Fig. 10. Illustration of S/N ratio. (a) Iteration 1, (b) Iteration 2, (c) Iteration 3, and (d) Iteration 4.

TABLE V
LEVELS OF CONTROL FACTORS

EF	Level	Iteration 1	Iteration 2	Iteration 3	Iteration 4
	1	2.65	3.05	3.25	3.35
S_1	2	3.05	3.25	3.35	3.40
	3	**3.45**	**3.45**	**3.45**	**3.45**
	1	3.40	3.60	3.70	3.75
S_2	2	**3.80**	**3.80**	**3.80**	**3.80**
	3	4.20	4.00	3.90	3.85
	1	**2.38**	2.38	2.48	2.58
S_3	2	2.78	**2.58**	2.58	**2.63**
	3	3.18	2.78	**2.68**	2.68
	1	1.57	1.77	1.97	2.07
S_4	2	**1.97**	1.97	2.07	2.12
	3	2.37	**2.17**	**2.17**	**2.17**

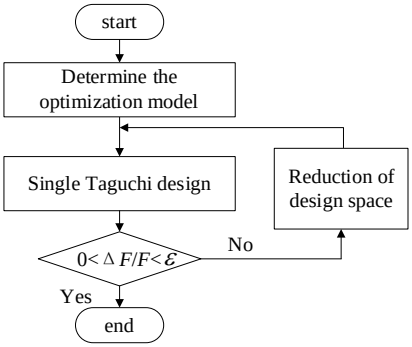

Fig. 11. Flowchart of sequential Taguchi method.

Step 7 Termination judgment.

The value of optimization function F is used to judge whether the selected EF combination meets the convergence condition. Iteration continues until the relative error of F between successive iterations is less than the specified threshold ε, which is set as 3% in this study. The value of F from iteration 1 should be compared with the initial design. If the relative error is smaller than ε and larger than 0, terminate the iteration progress and output the optimal EF sequence. Otherwise, reduce the design space and start another iteration.

The space reduction method is defined as follows. Assume the initial design space of a control factor is [a, b], including three levels with a step size of d. It is noteworthy that the step size will be halved during the space reduction. If the optimal level is x_0, then the designed levels for the same control factor in the next iterative process are determined by

$$\begin{cases} (a, a+d/2, a+d), & x_0 - d/2 < a \\ (b-d, b-d/2, b), & x_0 + d/2 > b \\ (x_0 - d/2, x_0, x_0 + d/2), & others \end{cases} \quad (12)$$

where d is the step size of the present iteration. The initial d is set as 0.4. The levels of control factors during the iteration are listed in Table V. Fig. 12 illustrates the robust EF sequence after 4 iterations. Actual values of robust EFs are listed in Table VI.

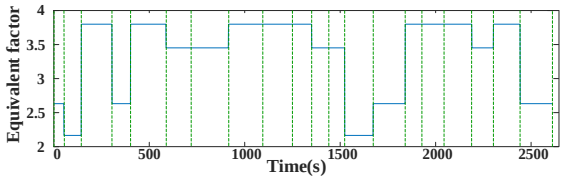

Fig.12. Robust EF sequence after 4 iterations.

TABLE VI
ROBUST SOLUTION

Segment type	1	2	3	4
EF	*S_1*	*S_2*	*S_3*	*S_4*
Value	3.45	3.80	2.63	2.17

D. *Performance evaluation*

Monte Carlo simulation (MCS) is employed to verify the effect of robust optimization. Latin hypercube sampling (LHS) is chosen as the sampling method to ensure the comprehensiveness of groups. Expectation and standard deviation of fuel consumption serve as evaluation indexes of robustness. The smaller expectation and standard deviation indicate that PHEB can maintain energy management effects under various driving conditions. Meanwhile, the distribution of soc_{end} is used as a failure measure for the upper limit of 35%. Too much battery power left indicates that the advantages of PHEB cannot be fully utilized. Despite conditions with uncertain factors smaller than nominal, most soc_{end} should be within the feasible region. The limit of soc_{end} and the objective of fuel economy are inherently non-conflicting.

IV. RESULTS AND DISCUSSION

A. *Results of deterministic and robust solutions*

Since the robust optimization is conducted based on deterministic design, a comparison between robust EF sequence and deterministic EF sequence is necessary, as listed in Table VII. It should be noted that the comparison is carried out under the constructed driving cycle with uncertainties set to their nominal values. Optimized by DP, deterministic EF sequence can achieve minimum fuel consumption. While the robust EF sequence consumes an additional 0.146L of fuel for considering the uncertainties. Besides, compared to the rule-based method and ECMS with fixed EF, segmented ECMS with robust EF sequence performs better. The final SOC of the robust EF sequence is 32.45% surpassing the lower limit of 30%. The SOC trajectories are similar, as shown in Fig. 13. Only a few points exhibit noticeable variations in machine torque on segment 13. On the other road segments machine torque curves are closer.

TABLE VII
COMPARISON UNDER DRIVING CYCLE WITH NOMINAL UNCERTAINTIES

Method	Fuel consumption	Final SOC
Deterministic EF sequence	19.19436	30.21%
Robust EF sequence	19.34034	32.45%
Fixed EF	20.16279	30.12%
Rule-based	22.13163	30.33%

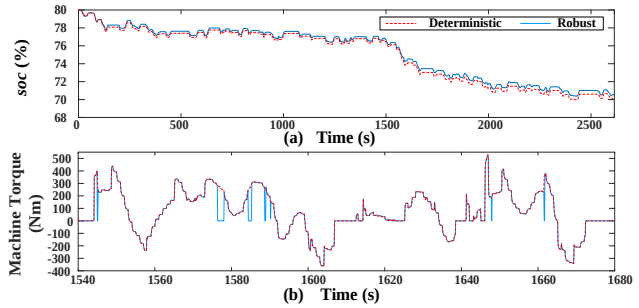

Fig.13. Comparison of simulation results (a) SOC trajectory, (b)Machine torque on segment 13.

B. Energy management performance in the face of uncertainties

The objective of robust optimization is to enhance overall fuel economy in the presence of uncertainties during actual driving. As a result, MCS is used to evaluate the performance of segmented ECMS. Fig. 14 illustrates the comparison of fuel consumption distribution. The distribution of the deterministic EF sequence reveals several clusters around 20L and 19L, whereas the robust EF sequence exhibits a peak value near 19.4L. Additionally, the deterministic results have a few test groups with fuel consumption exceeding 22L. While the highest fuel consumption in the robust results is 21.69L.

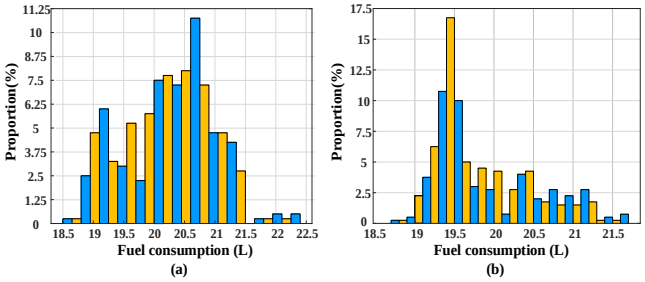

Fig.14. Distribution of fuel consumption. (a) Deterministic, (b) Robust.

Table VIII lists the actual fuel consumption expectations and standard deviation. The fuel consumption expectation of the robust EF sequence decreased by 0.3902L, equivalent to a reduction of 1.93%, compared with the deterministic EF sequence. Under the conditions of the city bus route and long-term operation, the overall fuel economy can be regarded as improved by robust optimization. Besides, the reduced standard deviation of the robust EF sequence indicates that the energy management system after robust optimization can keep good control effects despite uncertainties.

TABLE VIII
EXPECTATION AND STANDARD DEVIATION OF FUEL CONSUMPTION

Fuel consumption	Deterministic	Robust
Expectation(L)	20.2550	19.8648
ΔExpectation(%)	-	-1.93%
Standard deviation	0.7327	0.6296

Most final SOC values can satisfy the design requirement, with nearly half of the test groups depleting the battery capacity, as shown in Fig. 15. Only 4.8% of the test groups end with SOC values exceeding 35%, and part of them are associated with extreme working conditions. Therefore, the robust EF sequence can be considered reliable without insufficient battery usage. This result aligns with the observed decrease in the fuel consumption expectation.

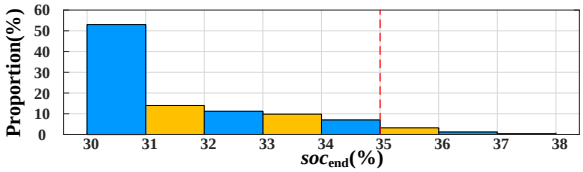

Fig.15. Distribution of soc_{end}.

C. HIL test

Hardware-in-the-loop (HIL) is an important testing method in the process of energy management control strategy development. By simulating the environment and using real hardware to form the HIL system, the real-time performance and reliability of the energy management strategy can be further verified. The HIL testing system built in this paper is mainly composed of the HIL testing cabinet, host computer, and physical controller, as shown in Fig. 16.

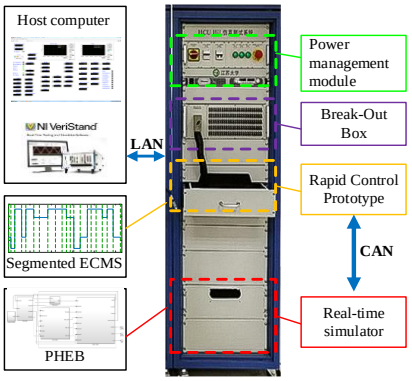

Fig.16. HIL testing platform.

The power management module supplies electricity for the HIL test cabinet and the real controller. The break-out box builds connections between the controller and test system, facilitating the independent extraction of each signal. The designed segmented ECMS with robust EF sequence is written into the rapid control prototype. The real-time simulator is used for simulating the PHEB model and sending dates to the host computer.

The HIL test results of the robust solution are shown in Fig. 17. The speed curve can track the constructed driving cycle of the city bus route well. Meanwhile, both the engine torque and the machine torque approximate the simulation results. The total fuel consumption is 19.37468L, close to the simulation result of 19.34034L, and the soc_{end} is 0.37% higher than 32.45%. According to the HIL test, the designed robust energy management strategy can be regarded as valid

and reliable.

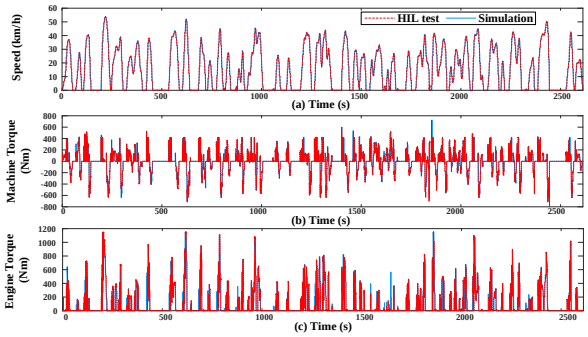

Fig.17. HIL test results. (a) Speed, (b) Machine torque, (c) Engine torque.

D. Discussion

The proposed robust optimization method is applied to the segmented ECMS, where the robust EF sequence enhances the effective control under uncertainties. From a theoretical perspective, the latest learning-based approaches have the potential to achieve similar robustness and near-global optimal performance. However, in practical application, the learning-based method faces challenges with design complexity and computational burden. In contrast, the proposed robust optimization method demonstrates superior overall performance in PHEB. Its advantages include ease of implementation, with the computationally intensive optimization process conducted offline, and the online use of ECMS providing strong real-time performance. The fixed routing of PHEB guarantees the potential for offline optimization as well.

V. CONCLUSION

This paper aims to improve the robustness of the energy management system for PHEB in the actual operation. Several uncertain factors that vary during the actual driving process are taken into account. The segmented ECMS is chosen as the basic control strategy, with EFs corresponding to each segment as optimization variables. Based on the result of deterministic optimization, a sequential Taguchi method is utilized for the robust optimization of control parameters. Results of MCS demonstrate that fuel consumption expectation of robust EF sequence decreases by 1.93% compared to the deterministic one. Given that the robust optimization is built upon the optimal fuel economy achieved through deterministic design, the reduction in fuel consumption is acceptable. This decrease comes from maintaining a strong control effect in the face of uncertain factors during actual driving. Especially in the case of long-term operation, a PHEB with robust ECMS can significantly reduce total fuel consumption.

To enhance robustness further, additional uncertain factors, such as the efficiencies of electronic components, can be incorporated into the optimization in future investigations. Moreover, the model predictive control can aid in addressing uncertainties related to speed on the basis of control parameter robust design.

REFERENCE

[1] X. Sun, Z. Jin, M. Xue, and X. Tian, "Adaptive ECMS with gear shift control by grey wolf optimization algorithm and neural network for plug-in hybrid electric buses," *IEEE Trans. Ind. Electron.*, vol. 71, no. 1, pp. 667-677, Jan. 2024.

[2] L. Li, X. Y. Wang, R. Xiong, K. He, and X. J. Li, "AMT downshifting strategy design of hev during regenerative braking process for energy conservation," *Appl. Energy,* vol. 183, pp. 914-925, Dec. 2016.

[3] X. Sun, Z. Dong, Z. Jin, G. Lei, and X. Tian, "System-level energy management optimization of power split hybrid electric vehicle based on nested design," *IEEE Trans. Ind. Electron.*, vol. 71, no. 9, pp. 10987-10997, Sep. 2024.

[4] L. Li, C. Yang, Y. Zhang, L. Zhang, "Correctional DP-based energy management strategy of plug-in hybrid electric bus for city-bus route," *IEEE Trans. Veh. Technol.,* vol. 64, no. 7, pp. 2792-2803, Jul. 2015.

[5] F. Wang, J. Xia, X. Zhu, X. Xu, and Y. Ni, "An online predictive energy management strategy for multi-mode plug-in hybrid electric vehicle with mode transition schedule optimization," *IEEE-ASME. T. Mech.*, to be published, DOI: 10.1109/TMECH.2023.3312259.

[6] R. Bagwe, A. Byerly, E. dos Santos, Jr., and Z. Ben-Miled, "Adaptive rule-based energy management strategy for a parallel HEV," *Energies*, vol. 12, no. 23, Dec. 2019.

[7] F. Qin, G. Xu, Y. Hu, K. Xu, and W. Li, "Stochastic optimal control of parallel hybrid electric vehicles," *Energies*, vol. 10, no. 2, Feb. 2017.

[8] L. Hao, Y. Wang, Y. Bai, and Q. Zhou, "Energy management strategy on a parallel mild hybrid electric vehicle based on breadth first search algorithm," *Energy Conv. Manag.*, vol. 243, Sep. 2021.

[9] S. Yang, J. Wang, F. Zhang, and J. Xi, "Self-adaptive equivalent consumption minimization strategy for hybrid electric vehicles," *IEEE Trans. Veh. Technol*., vol. 70, no. 1, pp. 189-202, Jan. 2021.

[10] F. Zhang, X. Hu, R. Langari, L. Wang, Y. Cui, and H. Pang, "Adaptive energy management in automated hybrid electric vehicles with flexible torque request," *Energy*, vol. 214, Jan. 2021.

[11] D. Shi, et al, "Deep reinforcement learning based adaptive energy management for plug-in hybrid electric vehicle with double deep Q-network," *Energy*, vol. 305, Art. no.: 132402, Jul. 2024.

[12] D. Biswas, S. Ghosh, S. Sengupta, and S. Mukhopadhyay, "Energy management of a parallel hybrid electric vehicle using model predictive static programming," *Energy,* vol. 250, Jul. 2022.

[13] J. Soldo, B. Skugor, and J. Deur, "Synthesis of optimal battery state-of-charge trajectory for blended regime of plug-in hybrid electric vehicles in the presence of low-emission zones and varying road grades," *Energies,* vol. 12, no. 22, Nov. 2019.

[14] J. Guo, H. He, J. Peng, and N. Zhou, "A novel MPC-based adaptive energy management strategy in plug-in hybrid electric vehicles," *Energy,* vol. 175, pp. 378-392, May. 2019.

[15] X. Sun, M. Xue, Y. Cai, X. Tian, Z. Jin, and L. Chen, "Adaptive ECMS based on EF optimization by model predictive control for plug-in hybrid electric buses," *IEEE Trans. Transport. Electrific.*, vol. 9, no. 2, pp. 2153-2163, Jun. 2023.

[16] J. Peng, H. He, and R. Xiong, "Rule based energy management strategy for a series-parallel plug-in hybrid electric bus optimized by dynamic programming," *Appl. Energy,* vol. 185, pp. 1633-1643, Jan. 2017.

[17] Z. Fang, Z. Chen, Q. Yu, and B. Zhang, "Online power management strategy for plug-in hybrid electric vehicles based on deep reinforcement learning and driving cycle reconstruction," *Green Energy Intell. Transp.*, vol. 1, no. 2, pp. 100016, Sep. 2022.

[18] D. Sun, X. Lin, D. Qin, and T. Deng, "Power-balancing instantaneous optimization energy management for a novel series-parallel hybrid electric bus," *Chin. J. Mech. Eng.,* vol. 25, no. 6, pp. 1161-1170, Nov. 2012.

[19] C. Zhang, Q. Zhou, M. Hua, H. Xu, M. Bassett, and F. Zhang, "Cuboid equivalent consumption minimization strategy for energy management of multi-mode plug-in hybrid vehicles considering diverse time scale objectives," *Appl. Energy,* vol. 351, Dec. 2023.

[20] R. Schmid, J. Buerger, and N. Bajcinca, "Energy management strategy for plug-in-hybrid electric vehicles based on predictive PMP," *IEEE Trans. Control Syst. Technol.,* vol. 29, no. 6, pp. 2548-2560, Nov. 2021.

[21] Z. Shen, C. Luo, and X. Dong, "Two-level energy control strategy based on ADP and A-ECMS for series hybrid electric vehicles," *IEEE Trans. Intell. Transp. Syst.,* vol. 23, no. 8, pp. 13178-13189, Aug. 2022.

[22] C. Yang, S. Du, L. Li, S. You, Y. Yang, and Y. Zhao, "Adaptive real-time optimal energy management strategy based on equivalent factors optimization for plug-in hybrid electric vehicle," *Appl. Energy*, vol. 203, pp. 883-896, Oct. 2017.

[23] X. Sun, Y. Cao, Z. Jin, X. Tian, and M. Xue, "An adaptive ECMS based on traffic information for plug-in hybrid electric buses," *IEEE Trans. Ind. Electron.*, vol. 70, no. 9, pp. 9248-9259, Sep. 2023.

[24] J. Shangguan, H. Guo, and M. Yue, "Robust energy management of plug-in hybrid electric bus considering the uncertainties of driving cycles and vehicle mass," *Energy,* vol. 203, Jul. 2020.

[25] D. Hou, Q. Dong, and Y. Zhou, "Taguchi robust design for adaptive energy management of plug-in fuel cell electric bus," *J. Energy Storage,* vol. 53, Sep. 2022.

[26] X. Sun, Z. Dong, Z. Jin, and X. Tian, "System-level energy management optimization based on external information for power-split hybrid electric buses," *IEEE Trans. Ind. Electron.*, to be published, DOI: 10.1109/TIE.2024.3370928.
[27] H. Guo, D. Hou, S. Du, and L. Zhao, "A driving pattern recognition-based energy management for plug-in hybrid electric bus to counter the noise of stochastic vehicle mass," *Energy,* vol. 198, May. 2020.
[28] H. Guo, B. Liang, H. Guo, and K. Zhang, "A robust co-state predictive model for energy management of plug-in hybrid electric bus," *J. Clean Prod.,* vol. 250, Mar. 2020.
[29] X. Liu, H. Guo, X. Cheng, J. Du, and J. Ma, "A robust design of the model-free-adaptive-control-based energy management for plug-in hybrid electric vehicle," *Energies,* vol. 15, no. 20, Oct. 2022.
[30] K. Diao, X. Sun, G. Lei, G. Bramerdorfer, Y. Guo, and J. Zhu, "System-level robust design optimization of a switched reluctance motor drive system considering multiple driving cycles," *IEEE Trans. Energy Convers.,* vol. 36, no. 1, pp. 348-357, Mar. 2021.
[31] K. Diao, X. Sun, G. Lei, G. Bramerdorfer, Y. Guo, and J. Zhu, "Robust design optimization of switched reluctance motor drive systems based on system-level sequential Taguchi method," *IEEE Trans. Energy Convers.,* vol. 36, no. 4, pp. 3199-3207, Dec. 2021.
[32] Y. Hong, A. Beltran, and A. Paglinawan, "A robust design of maximum power point tracking using Taguchi method for stand-alone PV system," *Appl. Energy,* vol. 211, pp. 50-63, Feb. 2018.
[33] R. Koubaa, S. Bacha, M. Smaoui, and L. Krichen, "Robust optimization based energy management of a fuel cell/ ultra-capacitor hybrid electric vehicle under uncertainty," *Energy,* vol. 200, Jun. 2020.
[34] X. Zhang, L. Yang, X. Sun, Z. Jin, and M. Xue, "ECMS-MPC energy management strategy for plug-in hybrid electric buses considering motor temperature rise effect," *IEEE Trans. Transp. Electrif.,* vol. 9, no. 1, pp. 210-221, Mar. 2023.

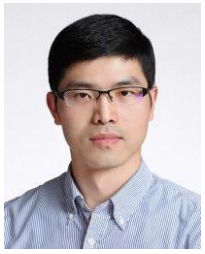

Xiaodong Sun (M'12-SM'18) received the B.Sc. degree in electrical engineering, and the M.Sc. and Ph.D. degrees in control engineering from Jiangsu University, Zhenjiang, China, in 2004, 2008, and 2011, respectively.

Since 2004, he has been with Jiangsu University, where he is currently a Professor in Vehicle Engineering with the Automotive Engineering Research Institute. From 2014 to 2015, he was a Visiting Professor with the School of Electrical, Mechanical, and Mechatronic Systems, University of Technology Sydney, Sydney, Australia. His current teaching and research interests include electrified vehicles, electrical machines, electrical drives, and energy management. He is the author or coauthor of more than 100 refereed technical papers and one book, and he is the holder of 42 patents in his areas of interest. Dr. Sun is an Associate Editor of the IEEE TRANSACTIONS ON INDUSTRIAL ELECTRONICS, Associate Editor of the IEEE TRANSACTIONS ON TRANSPORTATION ELECTRIFICATION, and Editor of the IEEE TRANSACTIONS ON ENERGY CONVERSION.

Zongzhe Chen was born in Yanchen, Jiangsu, China, in 2000. He received the B. S. degree in vehicle engineering from Jiangsu University, Zhenjiang, China, in 2022, and he is currently working toward the M.S. degree in Jiangsu University, Zhenjiang, China.

His current research interests include optimal design, energy management strategy, hybrid electric vehicles, and power-split powertrain control.

Mingzhang Pan received the Ph.D. degree in power machinery and engineering from the Tianjin University, Tianjin, China, in 2014. From 2014 to 2016, he worked as a postdoctoral researcher at Tianjin University. From 2017 to 2019, he worked as a postdoctoral researcher at Zhejiang University. Since 2016, he has been engaged in teaching and scientific research at the School of Mechanical Engineering, Guangxi University. His current teaching and research interests include internal-combustion engine, hybrid electric vehicle, power system control technology, and energy management.

Yingfeng Cai received the B.S., M.S., and Ph.D. degrees from the School of Instrument Science and Engineering, Southeast University, Nanjing, China. In 2013, she joined the Automotive Engineering Research Institute at Jiangsu University, where she is currently working as a Professor. Her research interests include computer vision, intelligent transportation systems, and intelligent automobiles. She got the National Fund for Distinguished Young Scholars of China.

Zhijia Jin (S'20) was born in Suzhou, Jiangsu, China, in 1994. He received the B.S. degree in vehicle engineering from Jiangsu University, Zhenjiang, China, in 2017, and he is currently working toward the Ph.D. degree in Jiangsu University, Zhenjiang, China.

His current research interests include design, optimization, magnetic equivalent circuits modeling, control, loss analysis of magnetic bearings and bearingless motors for flywheel energy storage system used in automobile application, hybrid electric vehicles, and vehicle powertrain control.

Gang Lei (M'14-SM'22) received the B.S. degree in Mathematics from Huanggang Normal University, China, in 2003, the M.S. degree in Mathematics and Ph.D. degree in Electrical Engineering from Huazhong University of Science and Technology, China, in 2006 and 2009, respectively.

He is currently a Senior Lecturer at the School of Electrical and Data Engineering, University of Technology Sydney (UTS), Australia. His research interests include computational electromagnetics, design optimization and control of electrical drive systems and renewable energy systems. He is an Associate Editor of the IEEE TRANSACTIONS ON INDUSTRIAL ELECTRONICS, Associate Editor of the IEEE TRANSACTIONS ON TRANSPORTATION ELECTRIFICATION, and Editor of the IEEE TRANSACTIONS ON ENERGY CONVERSION.

Xiang Tian received the B.S. degree in electrical engineering, M.S. degree in power electronics and power transmission and Ph.D. degree in vehicle engineering from Jiangsu University, Zhenjiang, China, in 2006, 2009 and 2018, respectively. He is currently a lecturer with the automotive engineering research institute, Jiangsu University.

His current research interests include electric vehicles, hybrid electric vehicles, parameter matching, optimal energy control strategy, and vehicle powertrain control.